A. Olah and P. v. R. Schleyer, Ed., Wiley, New York, N.Y., 1970, p 837.

(4) G. A. Olah, R. H. Schlosberg, R. D. Porter, Y. K. Mo, D. P. Kelly, and G. D. Mateescu, *J. Am. Chem. Soc.*, **94**, 2034 (1972).

(5) G. A. Olah, G. D. Mateescu, and Y. K. Mo, *J. Am. Chem. Soc.*, **95**, 1865 (1973).

(6) V. A. Koptyug, I. S. Isaev, and A. I. Rezvukhin, *Tetrahedron Lett.*, 823 (1967).

(7) For recent studies indicating the relationship between charge density and ^{13}C chemical shifts see (a) J. B. Stothers, "Carbon-13 NMR Spectroscopy", Academic Press, New York, N.Y., 1972, and references cited therein; (b) G. A. Olah, H. C. Lin, and D. A. Forsyth, *J. Am. Chem. Soc.*, **96**, 6809 (1974); (c) G. A. Olah, P. W. Westerman, and D. A. Forsyth, *ibid.*, **97**, 3419 (1975); (d) D. A. Forsyth, R. J. Spear, and G. A. Olah, *ibid.*, **98**, 2512 (1976).

(8) For an extensive survey of the theory and applications of dynamic nuclear magnetic resonance spectroscopy see L. M. Jackman and F. A. Cotton, Ed., "Dynamic Nuclear Magnetic Resonance Spectroscopy", Academic Press, New York, N.Y., 1975.

(9) The preparation of the benzenium ion from the dealkylation of *tert*-butylbenzene in SbF_5–FSO_3H–SO_2ClF solution was also studied by Dr. Y. K. Mo in our laboratories.

(10) J. P. Wibaut and F. A. Haak, *Recl. Trav. Chim. Pays-Bas*, **69**, 1387 (1950).

(11) W. J. Hehre and J. A. Pople, *J. Am. Chem. Soc.*, **94**, 690 (1972).

(12) D. H. O'Brien, A. J. Hart, and C. R. Russell, *J. Am. Chem. Soc.*, **97**, 4410 (1975).

(13) For extensive discussions of the concept of homoaromaticity, homoaromatic character, and homoaromatic compounds see (a) S. Winstein, *Q. Rev., Chem. Soc.*, **23**, 141 (1969); *Chem. Soc., Spec. Publ.*, **No. 21**, 5 (1967); (b) P. R. Story and B. C. Clark, Jr., in "Carbonium Ions", Vol. 3, G. A. Olah and P. v. R. Schleyer, Ed., Wiley, New York, N.Y., 1972, p 1007.

(14) G. A. Olah, J. S. Staral, R. J. Spear, and G. Liang, *J. Am. Chem. Soc.*, **97**, 5489 (1975).

(15) (a) P. Warner, D. L. Harris, C. H. Bradley, and S. Winstein, *Tetrahedron Lett.*, 4013 (1970); (b) P. Ahlberg, D. L. Harris, M. Roberts, P. Warner, P. Seidl, M. Sakai, D. Cook, A. Diaz, J. P. Dirlam, H. Hamberger, and S. Winstein, *J. Am. Chem. Soc.*, **94**, 7063 (1972); (c) W. J. Hehre, *ibid.*, **96**, 5207 (1974).

(16) (a) P. Warner and S. Winstein, *J. Am. Chem. Soc.*, **93**, 1284 (1971); (b) L. A. Paquette, M. J. Broadhurst, P. Warner, G. A. Olah, and G. Liang, *ibid.*, **95**, 3386 (1973).

(17) G. A. Olah and D. A. Forsyth, *J. Am. Chem. Soc.*, **97**, 3137 (1975).

(18) Chemical shifts taken from ref 7a and 37 were converted to parts per million relative to external Me_4Si utilizing δ_{13C} (external) = δ_{13C} (internal) + 1.0.

(19) A. Streitwieser, Jr., "Molecular Orbital Theory for Organic Chemists", Wiley, New York, N.Y., 1971.

(20) G. A. Olah, G. Liang, and S. P. Jindal, *J. Org. Chem.*, **40**, 3259 (1975).

(21) N. C. Baenziger and A. D. Nelson, *J. Am. Chem. Soc.*, **90**, 6602 (1968).

(22) V. A. Koptyug, I. K. Korobeinicheva, T. P. Andreeva, and V. A. Bushmelev, *Zh. Obshch. Khim.*, **38**, 1979 (1968).

(23) (a) N. Muller, W. Pickett, and R. S. Mulliken, *J. Am. Chem. Soc.*, **76**, 4770 (1954); (b) W. C. Ermler, R. S. Mulliken, and E. Clementi, *ibid.*, **98**, 388 (1976).

(24) G. A. Olah and R. D. Porter, *J. Am. Chem. Soc.*, **93**, 6877 (1971).

(25) G. A. Olah and R. J. Spear, *J. Am. Chem. Soc.*, **97**, 1539 (1975).

(26) W. Kitching, M. Bullpitt, D. Doddrell, and W. Adcock, *Org. Magn. Reson.*, **6**, 289 (1974).

(27) R. S. Ozubko, G. W. Buchanan, and I. C. P. Smith, *Can. J. Chem.*, **52**, 2493 (1974).

(28) (a) B. Birdsall, N. J. M. Birdsall, and J. Feeney, *J. Chem. Soc., Chem. Commun.*, 316 (1972); (b) B. Birdsall and J. Feeney, *J. Chem. Soc., Perkin Trans. 2*, 1643 (1972).

(29) In $CDCl_3$ solution at ambient temperature.

(30) R. LaLande and R. Calas, *Bull. Soc. Chim. Fr.*, 751 (1958).

(31) G. A. Olah, *J. Am. Chem. Soc.*, **86**, 932 (1964).

(32) D. M. Brouwer and J. A. Van Doorn, *Recl. Trav. Chim. Pays-Bas*, **89**, 88 (1970).

(33) The 300-MHz ^1H NMR spectra of 3 were obtained through the courtesy of Varian Associates.

(34) L. M. Jackman and S. Sternhell, "Applications of Nuclear Magnetic Resonance Spectroscopy in Organic Chemistry", 2nd ed, Pergamon Press, Elmsford, N.Y., 1969.

(35) (a) R. H. Martin, H. Defay, and F. Greets-Evrard, *Tetrahedron*, **20**, 1505 (1964); (b) G. O. Dudek, *Spectrochim. Acta*, **19**, 691 (1963).

(36) G. A. Olah, P. W. Westerman, and J. Nishimura, *J. Am. Chem. Soc.*, **96**, 3548 (1974).

(37) M. L. Caspar, J. B. Stothers, and N. K. Wilson, *Can. J. Chem.*, **53**, 1958 (1975).

(38) W. Adcock, M. Aurangzeb, W. Kitching, N. Smith, and D. Doddrell, *Aust. J. Chem.*, **27**, 1817 (1974).

(39) G. J. Ray, R. J. Kurland, and A. K. Colter, *Tetrahedron*, **27**, 735 (1971).

(40) R. W. Taft, Jr., N. C. Deno, and P. S. Skell, *Annu. Rev. Phys. Chem.*, **9**, 287 (1958).

(41) G. A. Olah, J. S. Staral, G. Liang, L. A. Paquette, W. P. Melega, and M. J. Carmody, *J. Am. Chem. Soc.*, **99**, 3349 (1977).

(42) D. L. Mackor, A. Hofstra, and J. H. van der Waals, *Trans. Faraday Soc.*, **54**, 186 (1958).

Dipole Moment, Optical Anisotropy, and Molar Kerr Constant of Triacetin

Wayne L. Mattice*[1] and Enrique Saiz[2]

Contribution from the Department of Chemistry, Louisiana State University, Baton Rouge, Louisiana 70803, and Department of Chemistry, Stanford University, Stanford, California 94305. Received January 14, 1978

Abstract: A rotational isomeric state treatment of unperturbed triacetin is presented. The objective is to determine conformational preferences of the glycerol moiety in unperturbed triglycerides. Calculations based on the model provide excellent agreement with the experimental dipole moment, optical anisotropy, and molar Kerr constant. The orientation of the ester group dipole moment and composition of the anisotropic part of the ester group polarizability tensor are among the critical parameters in the calculation. Experimental results are reproduced using values for these parameters which differ only slightly from those utilized successfully for methyl acetate. Statistical weights deduced from the analysis reveal that a variety of configurations are accessible to the glycerol moiety in an unperturbed triglyceride. Among the accessible configuration is the one adopted by β-tricaprin and β-trilaurin in the crystalline state. About 1% of the triacetin molecules exist with the glycerol moiety in this configuration. Certain other configurations are ten times more prevalent than the one found in the crystalline state.

Lipids derived from glycerol are important components of biological membranes.[3,4] They also occur in complexes with specific proteins in solution.[5] Depending upon temperature, their conformational freedom may either be severely restricted or they may exist in a fluid environment. Reversible transitions between these two states have been characterized by a variety of techniques. The temperature at which lipid components of membranes undergo the transition depends upon the chain length and extent of unsaturation of fatty acids esterified to the glycerol moiety.[3,4] Models have been proposed which view the hydrocarbon portion as a rigid planar zigzag below the

transition temperature. Disorder is introduced at higher temperatures, perhaps via the presence of a single bond in a gauche state[6] or a β-coupled gauche kink.[7] More extensively disordered states are also likely to be present. Three rotational states for each single bond about which rotation can occur would dictate 10^{25} configurations for unperturbed tristearin.

Configurational properties for unperturbed molecules which possess such a large number of configurations are most conveniently handled using rotational isomeric state theory.[8,9] This approach would be most appropriate for the bulk amorphous
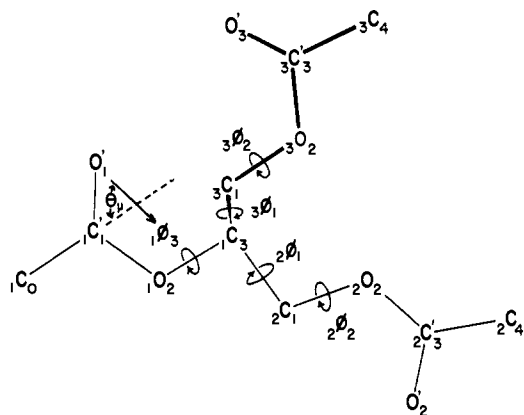
Figure 1. Structure of triacetin. Hydrogen atoms have been omitted.

Figure 2. View along the following bond vectors: (a) $_1l_3$ when $_1\phi_3 = 0°$ (trans state). (b) $_2l_1$ when $_2\phi_1 = 0°$ (trans state). (c) $_3l_1$ when $_3\phi_1 = 0°$ (trans state).

Table I. Bond Lengths and Angles

bond length, Å		bond angle, deg	
C–C	1.51	∠CC′O′	126.3
C–C′	1.50	∠OC′O′	122.3
C–O	1.44	∠COC′	116.7
C′–O	1.35	∠CCC	114.7
C′–O′	1.20	∠OCC	106.4

lipid or for the lipid when present in an ideal solution. Biological membranes are not likely to precisely fulfill either of these conditions. However, the configurational properties deduced by rotational isomeric state theory for the unperturbed state should serve as an instructive approximation to the lipids when they are above the transition temperature. Certainly the unperturbed state is more relevant than the crystalline state at such temperatures. A major difficulty in the development of a satisfactory rotational isomeric state treatment of lipids derived from glycerol is presented by the glycerol moiety itself. It is most conveniently viewed as containing a trifunctional branch point, requiring utilization of rotational isomeric state theory in the form appropriate for branched molecules.[10,11] Our present objective is to describe a rotational isomeric state treatment of triacetin which provides agreement with the observed dipole moment, optical anisotropy, and molar Kerr constant.

Conformational Energy Calculations

Structure. The triacetin molecule, depicted in Figure 1, consists of three branches which meet at the β carbon atom of the glycerol moiety. That portion bonded to the branch point via a C–O bond is designated as branch 1, the remaining two branches being 2 and 3. Chain atoms, bond vectors, and dihedral angles are numbered consecutively within each branch.[10] Numbering for branch 1 commences at the end remote from the branch point; for the other two branches numbering commences at the branch point. Atom, bond vector, and dihedral angle i in branch j are denoted by $_jA_i$, $_jl_i$, and $_j\phi_i$, respectively, and n_j is the number of bonds in branch j. Atoms in the carbonyl group are denoted by primes. A single subscript is used for the carbonyl oxygen atom. Bond lengths and bond angles are those found in crystalline β-tricaprin[12] (Table I). The C–H bond length was taken to be 1.00 Å.

Potential Functions. The 6–12 potentials were formulated as for poly(L-lactic acid).[13] Torsional potentials for C–O and C–C bonds were those used for poly(L-lactic acid)[13] and polymethylene,[14] respectively. Electric dipole moments for the ester groups were assigned a magnitude of 1.77 D and an angle θ_μ with the C′–C bond (Figure 1). The probable range for θ_μ
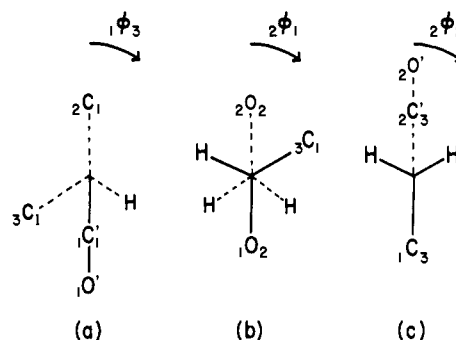
is 60–80°.[15] Electrostatic energies were evaluated in the monopole approximation, using a dielectric constant of 2–5.[13] Partial charges were selected which reproduce the magnitude and assigned orientation of the ester group dipole moment.

Rotational States. Ester groups were maintained in the planar trans conformation ($_1\phi_2 = _2\phi_3 = _3\phi_3 = 0°$) because of the high energy of the cis conformation.[16]

Figure 2(a) shows a view along $_1l_3$. The trans (t) state for this bond is defined as the low-energy region where $_1C_1′$, $_1O_2$, $_1C_3$, and $_2C_1$ are nearly coplanar trans, while the gauche$^+$ (g$^+$) state is produced when the first three of these atoms and $_3C_1$ are nearly coplanar trans. Values of 0 and 122.7° would be assigned to $_1\phi_3$ for these states if precise coplanarity was demanded. Such circumstances produce an interatomic distance of only 2.65 Å for $_1O′$ and either $_3C_1$ or $_2C_1$. Nonbonded interaction of carbonyl oxygen atom and methylene group is nearly 4 kcal/mol at this separation. Repulsion can be reduced by an increase in $_1\phi_3$ for the t state or a corresponding decrease for the g$^+$ state. No relief is possible in the g$^-$ state, as is evident from inspection of Figure 2(a). These considerations cause dihedral angles of Δ_1, 122.7° $- \Delta_1$, and 241.35° to be assigned to t, g$^+$, and g$^-$ states (Δ_1 is positive).

A view along $_2l_1$ is shown in Figure 2(b). The trans state is obtained when $_1O_2$, $_1C_3$, $_2C_1$, and $_2O_2$ are nearly coplanar trans. An internuclear separation of 2.92 Å is obtained for $_2O_2$ and $_3C_1$ when this group of atoms is precisely coplanar. Relief from the small repulsive interaction is obtained by placing the trans state at $_2\phi_1 = -\Delta_2$ (Δ_2 is positive). Similar consideration of the interaction of $_2O_2$ and $_3O_2$ in the g$^-$ state suggests that $_2\phi_1$ for this state should be displaced by Δ_3 from the value which produces a trans arrangement for $_2O_2$, $_2C_1$, $_1C_3$, and $_3C_1$. These considerations locate t, g$^+$, and g$^-$ states for $_2\phi_1$ at $-\Delta_2$, 121.35° $+ \Delta_2 - \Delta_3$, and 242.7° $+ \Delta_3$. The zero for $_3\phi_1$ is obtained when $_1O_2$, $_1C_3$, $_3C_1$, and $_3O_2$ are planar trans. The t, g$^+$, and g$^-$ states are located at Δ_2, 117.3° $- \Delta_3$, and 238.65° $- \Delta_2 + \Delta_3$.

Figure 2(c) presents the view along $_2l_2$. Interaction of $_1C_3$ with $_2O′$ in the g$^\pm$ states is similar to that described in conjunction with the t and g$^+$ states for the last bond in branch 1. Rotational states for the second bond in branches 2 and 3 therefore occur at 0° and $\pm(122.7° - \Delta_1)$.

Figure 3 depicts the manner in which conformational energy depends on $_1\phi_3$ and $_2\phi_1$. Location of the six minima suggests $\Delta_1 = 20–30°$, $\Delta_2 = 5–10°$, and $\Delta_3 = 0–5°$. The g$^-$ state is untenable for the last bond in branch 1 because of the inability to relieve severe steric interaction of $_1O′$ with both $_2C_1$ and $_3C_1$. This conclusion is in harmony with conformational energy surfaces reported by McAlister et al.[17] for the analogous portion of a lecithin. The essential features of Figure 3 are not significantly modified by reasonable changes in dielectric constant or orientation of the ester group dipole moment.
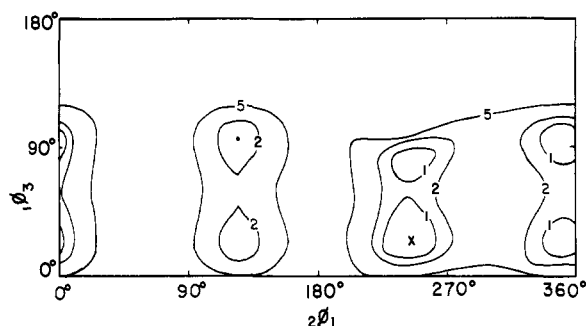
Figure 3. Conformational energy for triacetin as a function of $_1\phi_3$ and $_2\phi_1$ ($\epsilon = 3.5$, $\theta_\mu = 80°$, and $_2\phi_2 = _3\phi_1 = _3\phi_2 = 0°$). Contour lines are drawn at 1, 2, and 5 kcal/mol above the minimum energy, which occurs at the site denoted by X. Energies in the vicinity of $_1\phi_3 = 240°$ are 10 kcal/mol or more above that found at X.

Statistical Weight Matrices. The configuration partition function, Z, is generated in the manner appropriate for a molecule containing a single trifunctional branch point.[10]

$$Z = {_1U_1}^{(3)}({_2U_1}\,\theta\,{_3U_1})[({_2U_2}^{(3)}) \otimes ({_3U_2}^{(3)})] \qquad (1)$$

The statistical weight matrix for bond i in branch j is $_jU_i$, symbolism of the type $_1U_1^{(3)}$ denotes the product of three successive statistical weight matrices, commencing with $_1U_1$,[8] $\otimes$ denotes the direct product, and $_2U_1\,\theta\,_3U_1$ denotes the rectangular matrix defined in ref 10. For triacetin $_1U_1 = _1U_2 = 1$. Deletion of the untenable g⁻ state leaves two states, t and g⁺, for the last bond in branch 1. The symmetry of triacetin dictates equal statistical weights for the t and g⁺ states, yielding

$$_1U_3 = [1 \quad 1] \qquad (2)$$

Atoms which participate in first-order interactions embodied in $_2U_1$ are shown in Figure 2(b). The t, g⁺, and g⁻ states find $_2O_2$ participating in an interaction with $_3C_1$, with both $_1O_2$ and $_3C_1$, and with $_1O_2$, respectively. The difference in energy of the g⁻ and t states ranges from -0.3 to 1.0 kcal/mol when $\theta_\mu = 60{-}80°$ and Δ_2 and Δ_3 are confined to their probable ranges. The stability of the g⁻ state may be underestimated because the potential functions used cannot account for the first-order interaction of oxygen atoms in poly(ethylene oxide).[18,19] We shall use σ_1 for the statistical weight of the t state, and estimate the corresponding energy to lie in the range ±1 kcal/mol. The statistical weight of the g⁺ state relative to the g⁻ state is σ_2. Energies in the g⁺ state exceed those in the g⁻ state by 0.3–1.2 kcal/mol when $\theta_\mu = 60{-}80°$ and Δ_2 and Δ_3 are restricted to their probable ranges.

A second-order interaction occurs between $_2O_2$ and $_1C_1'$ (and, to a lesser extent, $_1C_1'$) when $_1\phi_3$, $_2\phi_1$ are in the g⁺g⁻ state. Variation of Δ_1 and Δ_3 over their probable ranges causes the $_2O_2{-}_1O'$ distance to vary from 2.25 to 2.57 Å, while the range for the $_2O_2{-}_1C_1'$ distance is 2.65–2.84 Å. Nonbonded interactions are repulsive for each interacting pair over the pertinent ranges. The total energy ranges from 1.3 to 9 kcal/mol, and gives rise to the statistical weight denoted ω_1. These considerations permit the formulation of $_2U_1$ as

$$_2U_1 = \begin{bmatrix} \sigma_1 & \sigma_2 & 1 \\ \sigma_1 & \sigma_2 & \omega_1 \end{bmatrix} \qquad (3)$$

Several interactions whose statistical weights occur in $_3U_1$ have already been discussed in connection with $_2U_1$. Additional interactions may occur between $_3O_2$ and $_2O_2$ when $_2\phi_1$, $_3\phi_1$ are in the tt or g⁺g⁻ states. The separation in the tt state is 2.66–2.78 Å and that in the g⁺g⁻ state is 2.50–2.69 Å when Δ_2 and Δ_3 are varied appropriately. Nonbonded and electrostatic interactions are repulsive under these circumstances,

giving rise to statistical weights ω_2 and ω_3 with estimated energies of 0–1 and 0.3–3 kcal/mol, respectively. Equation 4 presents the final expression for $_2U_1\,\theta\,_3U_1$.

$$_2U_1\,\theta\,_3U_1 =$$
$$\begin{bmatrix} \sigma_1^2\omega_2 & \sigma_1\omega_1 & \sigma_1\sigma_2 & \sigma_1\sigma_2 & \sigma_2\omega_1 & \sigma_2^2\omega_3 & \sigma_1 & \omega_1 & \sigma_2 \\ \sigma_1^2\omega_2 & \sigma_1 & \sigma_1\sigma_2 & \sigma_1\sigma_2 & \sigma_2 & \sigma_2^2\omega_3 & \sigma_1\omega_1 & \omega_1 & \sigma_2\omega_1 \end{bmatrix}$$
$$\qquad (4)$$

Atoms involved in interactions which depend only on $_2\phi_2$ are shown in Figure 2(c). The most important interactions in the g± states are between $_1C_3$ and its attached hydrogen atom and both $_2C_3'$ and $_2O'$. A contribution also arises from the torsional potential. The magnitude of individual interactions ranges from -0.1 to 0.5 kcal/mol for the appropriate values of Δ_1. In aggregate the estimated energy might be as large as 1 kcal/mol; the statistical weight is σ_3. Four combinations of $_2\phi_1$ and $_2\phi_2$ (tg⁻, g⁺g±, g⁻g⁺) produce interactions between $_2O'$ and either $_1O_2$ or $_3C_1$. Atom $_2C_3'$ participates in these interactions to a lesser extent. Calculated energies range upward from 2 kcal/mol. The statistical weight for these second-order interactions is ω_4. This interaction also occurs when $_3\phi_1$ and $_3\phi_2$ are tg⁺, g⁺g⁻, or g⁻g±. Complete expressions for $_2U_2$ and $_3U_2$ are

$$_2U_2 = \begin{bmatrix} 1 & \sigma_3 & \sigma_3\omega_4 \\ 1 & \sigma_3\omega_4 & \sigma_3\omega_4 \\ 1 & \sigma_3\omega_4 & \sigma_3 \end{bmatrix} \qquad (5)$$

$$_3U_2 = \begin{bmatrix} 1 & \sigma_3\omega_4 & \sigma_3 \\ 1 & \sigma_3 & \sigma_3\omega_4 \\ 1 & \sigma_3\omega_4 & \sigma_3\omega_4 \end{bmatrix} \qquad (6)$$

Remaining statistical weight matrices for triacetin are $_2U_3 = _3U_3 = \text{col}(1, 1, 1)$ and $_2U_2 = _3U_4 = 1$.

Third-order interactions can be generated by appropriate combinations of three successive dihedral angles. Necessary pairs of consecutive dihedral angles are suppressed by interactions considered above.

Configuration-Dependent Properties

Dipole Moment. Experimental values for the mean-square dipole moment, $\langle\mu^2\rangle$, are in the range 7.3–8.2 D² for tripalmitin and tristearin in benzene.[20-23] Slightly higher values, 8.6–8.9 D², were obtained in dioxane.[22,23] These results encompass a range of 8.1 ± 0.8 D². This range will be assumed to apply also to triacetin because the dipole moment arises from the ester groups, and the relative orientations of the esters in the unperturbed state should be arises from the ester groups, and the relative orientations of the esters in the unperturbed state should be unaffected by lengthening of the hydrocarbon portion of the acyl groups.

The mean-square dipole moment could be calculated using generator matrices constructed according to eq 39 of ref 11. We prefer to evaluate μ^2 for each of the 162 configurations and then average according to the statistical weights just described. This procedure permits evaluation of the distribution for μ^2 as well as $\langle\mu^2\rangle$. For each configuration μ^2 is obtained as $\mu^T\mu$, where μ is the vector obtained by appropriate summation of the ester group dipole moment vectors, and μ^T is the transpose of μ.

Optical Anisotropy. Measurements of depolarized Rayleigh scattering[24,25] at 632.8 nm (He–Ne laser) were carried out at 25 °C for carbon tetrachloride solutions containing volume fractions of triacetin (Sigma Chemical Co.) ranging from 0.10 to 0.50. Apparent values, $\langle\gamma^2\rangle_{app}$, were obtained at each concentration after correction for induced scattering on the basis of depolarized Rayleigh scattering intensities observed

Table II. Summary of Parameters[a]

parameter	ref value	probable range	effect of variation[b] $\langle\mu^2\rangle$	$\langle\gamma^2\rangle$	$\langle mK\rangle$
E_{σ_1}	-0.5	+1	-0.4	-0.9	2.7
E_{σ_2}	1.1	0.75 ± 0.45	0.5	0.1	0.0
E_{σ_3}	0.2	0.7 ± 0.3	-2.8	-0.1	-1.4
E_{ω_1}	2.0	1.3<	0.0	0.0	0.0
E_{ω_2}	0.0	0.5 ± 0.5	0.1	-0.6	1.1
E_{ω_3}	2.0	0.3<	0.0	0.0	0.0
E_{ω_4}	2.0	2<	0.0	0.0	0.0
Δ_1	20	25 ± 5	-0.7	-0.2	-1.1
Δ_2	5	7.5 ± 2.5	-0.1	-0.1	0.1
Δ_3	0	2.5 ± 2.5	0.0	0.0	0.1
θ_μ	82	70 ± 10	1.6		1.0
θ_α	0	0 ± 10		0.1	0.3
Γ_{CC}	0.54	0.54 ± 0.05		0.0	0.0
$\Delta\alpha$	0.48	0.45 ± 0.10		0.7	-1.9
$\Delta\alpha^\dagger$	1.22	1.35 ± 0.05		0.6	0.6

[a] Energies in kcal/mol, angles in degrees, components of polarizability tensors in Å^3, $\langle\mu^2\rangle$ in D^2, $\langle\gamma^2\rangle$ in Å^6, and $\langle mK\rangle$ in 10^{10} cm^5 statvol^{-2} mol^{-1}. [b] Change in $\langle\mu^2\rangle$, $\langle\gamma^2\rangle$, or $\langle mK\rangle$ when the indicated parameter is varied over the range denoted by column 3, all other parameters having the value in column 2. A negative sign is present if $\langle\mu^2\rangle$, $\langle\gamma^2\rangle$, or $\langle mK\rangle$ decrease when the variable parameter increases.

using two interferometric filters with bandwidths of 18 and 53 cm^{-1}. Attenuation factors for the central component (intrinsic or rotational component) were set equal to unity.[26] Intrinsic molecular anisotropy was evaluated by extrapolation of $\langle\gamma^2\rangle_{app}$ to infinite dilution, giving $\langle\gamma^2\rangle = 3.8 \pm 0.3 \text{ Å}^6$.

Each configuration has γ^2 given by

$$\gamma^2 = 1.5 \text{ trace } (\hat{\alpha}\hat{\alpha}) \qquad (7)$$

where $\hat{\alpha}$ is the anisotropic part of the polarizability tensor for triacetin in that configuration. This tensor can be obtained as

$$\hat{\alpha} = \hat{\alpha}_P + \sum_{i=1}^{3} T_i\hat{\alpha}_{MA}T_i^T - 3\,\hat{\alpha}_{CH_4} \qquad (8)$$

where subscripts P, MA, and CH$_4$ refer to propane, methyl acetate, and methane, respectively. The carbon atoms in propane will become the carbon atoms of the glycerol moiety. Three molecules of methyl acetate are rotated so that they have the geometric relationship to propane which the ester groups have with respect to the glycerol moiety in triacetin. This transformation is achieved using the T_i, whose construction depends on the configuration for which $\hat{\alpha}$ is desired. Addition of $\hat{\alpha}_P$ and the three transformed $\hat{\alpha}_{MA}$, followed by subtraction of tensors for three molecules of methane (which is isotropic), yields $\hat{\alpha}$ for triacetin in the desired configuration. Anisotropic parts of the polarizability tensor for propane and methyl acetate are

$$\hat{\alpha}_P = \Gamma_{CC} \text{ diag } (0.75, -0.08, -0.67) \qquad (9)$$

$$\hat{\alpha}_{MA} = (\Delta\alpha/3) \text{ diag } (2, -1, -1)$$
$$+ (\Delta\alpha^\dagger/2) \text{ diag } (0, 1, -1) \qquad (10)$$

The coordinate system in which $\hat{\alpha}_P$ is expressed has its x axis through the terminal carbon atoms and the y axis in the plane of the three carbon atoms. Depolarized Rayleigh scattering of n-alkanes requires $\Gamma_{CC} = 0.54 \pm 0.05 \text{ Å}^3$.[24] The coordinate system in which $\hat{\alpha}_{MA}$ is expressed has its x axis along the C–C′ bond and the y axis in the ester plane.[27] Rotation of the principal axes in the ester plane is denoted by θ_α. Measured γ^2 and molar Kerr constants for methyl acetate are reproduced with θ_α close to zero, $\Delta\alpha = 0.45 \pm 0.10 \text{ Å}^3$, and $\Delta\alpha^\dagger = 1.35 \pm 0.05$ Å^3.[27] Of course, $\hat{\alpha}_{CH_4}$ is diag (0, 0, 0). Averaging of the 162 γ^2 to yield $\langle\gamma^2\rangle$ is accomplished as for $\langle\mu^2\rangle$.
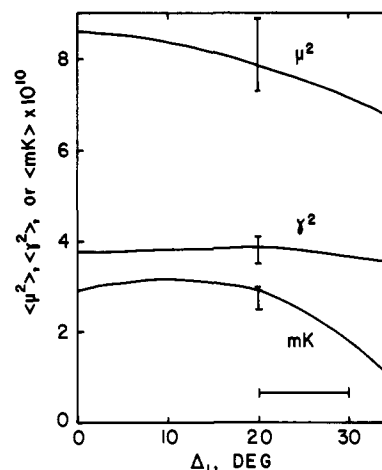

Figure 4. Sensitivity of $\langle\mu^2\rangle$, $\langle\gamma^2\rangle$, and $\langle mK\rangle$ to the assignment of Δ_1. All other parameters have their reference values. The probable range for Δ_1 is denoted by a horizontal bar. Vertical bars correspond to the range of measured values. They are drawn at the reference value for Δ_1.

Molar Kerr Constant. Electric birefringence of carbon tetrachloride solutions was measured at 25 °C using radiation from a He–Ne laser (632.8 nm); volume fractions of triacetin ranged from 0.03 to 0.13. The molar Kerr constant, $\langle mK\rangle$, at infinite dilution is given by[26,28]

$$\langle mK\rangle = 54\lambda\tilde{n}(n^2 + 2)^{-2}(\epsilon + 2)^{-2}$$

$$\times \left[\lim_{m\to 0} (\Delta B/m) + V^0B^0\right] \qquad (11)$$

where $\tilde{n}$, ϵ, V^0, and B^0 are respectively the refractive index, dielectric constant, molar volume, and electric birefringence of the solvent; $\Delta B = B - B^0$ is the difference in birefringence between a solution of molar concentration m and that of the pure solvent. The result of this extrapolation is $\langle mK\rangle = 2.75 \pm 0.25 \times 10^{-10}$ cm^5 statvol^{-2} mol^{-1}.

The molar Kerr constant for each configuration of triacetin is obtained from[8]

$$mK = (2\pi N_A/15kT)[\mu^T\hat{\alpha}\mu(kT)^{-1} + (2.2/3)\gamma^2] \qquad (12)$$

Here μ and $\hat{\alpha}$ are expressed in the same coordinate system, and it is assumed that the static polarizability tensor is 10% larger than the optical polarizability tensor. Averaging is accomplished as for $\langle\mu^2\rangle$ and $\langle\gamma^2\rangle$.

Influence of the Location of Rotational States. Orientation of the Ester Group Dipole Moment, and Composition of the Anisotropic Part of the Polarizability Tensor

Calculations require assignment of values to the parameters listed in Table II. Sensitivity of $\langle\mu^2\rangle$, $\langle\gamma^2\rangle$, and $\langle mK\rangle$ to the assignments is best presented by first defining a reference set of values (second column of Table II). This set yields $\langle\mu^2\rangle = 7.86 \text{ D}^2$, $\langle\gamma^2\rangle = 3.83 \text{ Å}^6$, and $\langle mK\rangle = 2.86 \times 10^{-10}$ cm^5/statvol^2 mol, in excellent agreement with the experimental values of $8.1 \pm 0.8 \text{ D}^2$, $3.8 \pm 0.3 \text{ Å}^6$, and $2.75 \pm 0.25 \times 10^{-10}$ cm^5/statvol^2 mol.

Location of Rotational States. Consequences of variation in Δ_1 are depicted in Figure 4 and summarized in Table II. The molar Kerr constant is particularly sensitive to Δ_1. Experimental values for $\langle\mu^2\rangle$ and $\langle mK\rangle$ are best reproduced if Δ_1 is placed at the lower end of its probable range. Little consequence attends adjustments of Δ_2 and Δ_3 (Table II).

Orientation of the Ester Group Dipole Moment. Dependence of $\langle\mu^2\rangle$ and $\langle mK\rangle$ on θ_μ is depicted in Figure 5. The mean-square dipole moment and molar Kerr constant increase as θ_μ increases. Reproduction of experimental values requires that
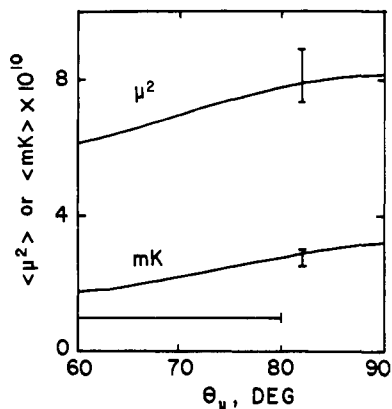
Figure 5. Sensitivity of $\langle\mu^2\rangle$ and $\langle mK\rangle$ to variation in θ_μ.
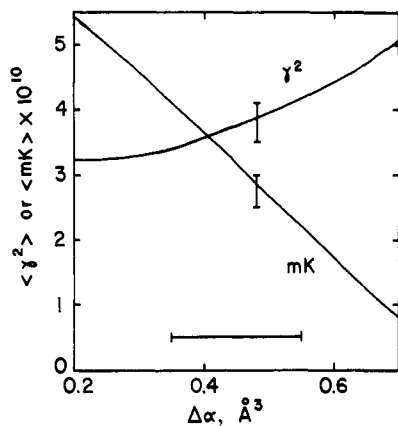

Figure 6. Effect of variation in $\Delta\alpha$ on $\langle\gamma^2\rangle$ and $\langle mK\rangle$.
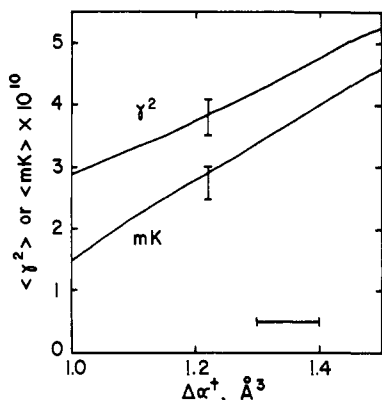

Figure 7. Effect of variation in $\Delta\alpha^\dagger$ on $\langle\gamma^2\rangle$ and $\langle mK\rangle$.

Figure 8. Distributions for μ^2 when all configurations are weighted equally (dashed lines) or according to the reference statistical weights (solid lines).

θ_μ be large. The reference value adopted lies slightly above the estimated probable range. However, θ_μ as low as 75° produce dipole moments and molar Kerr constants within the experimental range.

Anisotropic Part of the Polarizability Tensor. Variation of Γ_{CC} within its probable range has little consequence (Table II). Computed results are insensitive to the uncertainty in $\hat{\alpha}_P$. In contrast, computed molar Kerr constants are particularly sensitive to reasonable variation in $\Delta\alpha$ and $\Delta\alpha^\dagger$ (Figures 6 and 7). Calculated molar Kerr constants are too large if $\Delta\alpha^\dagger$ is restricted to its probably range. However, a slight decrease in $\Delta\alpha^\dagger$ causes it to move into the experimental range. Optical
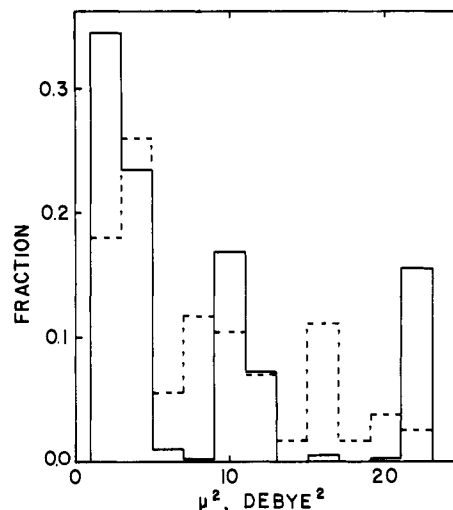
anisotropies are also sensitive to $\Delta\alpha$ and $\Delta\alpha^\dagger$, but less so than is the molar Kerr constant. Values of $\Delta\alpha$ and $\Delta\alpha^\dagger$ which reproduce the experimental $\langle mK\rangle$ also provide agreement with the experimental $\langle\gamma^2\rangle$. Small rotations of the principal axes in the plane of the ester group have little effect on $\langle\gamma^2\rangle$ and $\langle mK\rangle$.

The most important of the adjustable parameters considered in this section are θ_μ, Δ_1, $\Delta\alpha$, and $\Delta\alpha^\dagger$. The reference values for θ_μ and Δ_1 were required in order to prevent the computed $\langle\mu^2\rangle$ being lower than that attained experimentally. Subsequent assignment of $\Delta\alpha$ and $\delta\alpha^\dagger$ is governed primarily by the need to bring the calculated molar Kerr constant into the experimental range.

Distributions for μ^2, γ^2, and mK if All Configurations Were Equally Probable

Individual configurations have μ^2 of 1.4–23.0 D^2. The latter result is close to the upper limit of 28.2 D^2 which would be attained if the three ester group dipole moments had identical orientations. The distribution for μ^2 is presented as the dashed line in Figure 8. Its maximum occurs at 4 D^2. Nearly half (44%) of the configurations have $\mu^2 < 5$ D^2. A similar fraction (43%) is spread over the range 12 ± 5 D^2. Equal weighting for all configurations yields $\langle\mu^2\rangle = 8.15$ D^2, which is within the range of values attained experimentally.

A range of 1.0–10.7 Å^6 is encompassed by γ^2 for individual configurations. The distribution is shown as the dashed line in Figure 9. A range of 2.5 ± 1.5 Å^6 accounts for $\frac{2}{3}$ of the configurations. Only 4% have $\gamma^2 > 8$ Å^6. Equal weights for all configurations yields $\langle\gamma^2\rangle = 3.61$ Å^6, which is within the range found experimentally.

Molar Kerr constants for individual configurations range from -8 to 25×10^{-10} cm^5/statvol^2 mol. Large values are attained in the configurations with the largest μ^2, i.e., those in which the three ester groups have nearly identical orientations in space. Slightly more than $\frac{2}{3}$ of the configurations have $mK = 3 \pm 6 \times 10^{-10}$ cm^5/statvol^2 mol (dashed line in Figure 10). The average value is 4.3×10^{-10} cm^5/statvol^2 mol, which exceeds the experimental result.

Consequences of the Statistical Weights

Figure 11 presents the manner in which variation in the energy associated with σ_1 affects $\langle\mu^2\rangle$, $\langle\gamma^2\rangle$, and $\langle mK\rangle$. Trends are susceptible to rationalization through reference to Table III. The six most probable configurations have statistical
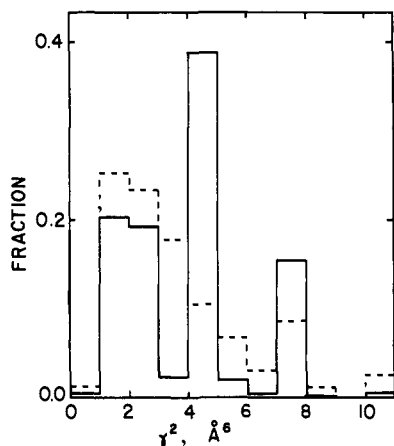
Figure 9. Distribution for γ^2 when all configurations are weighted equally (dashed) or according to the reference statistical weights (solid).
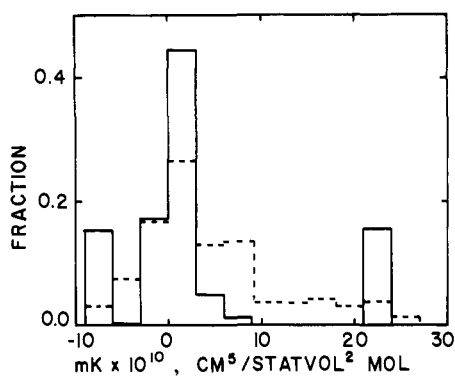

Figure 11. Effect of variation in $E_{\sigma 1}$ on $\langle \mu^2 \rangle$, $\langle \gamma^2 \rangle$, and $\langle mK \rangle$.

Figure 10. Distributions for mK when all configurations are weighted equally (dashed) or according to the reference statistical weights (solid).

Figure 12. Effect of variation in $E_{\sigma 3}$ on $\langle \mu^2 \rangle$, $\langle \gamma^2 \rangle$, and $\langle mK \rangle$.

Table III. Summary of the 16 Most Prevalent Configurations[a]

statistical weight	statistical weight/Z^b	μ^2	γ^2	mK
$\sigma_1{}^2\omega_2$	0.107	1.6	4.2	0.3
$\sigma_1{}^2\sigma_3\omega_2$	0.076	4.7	7.5	−0.9
$\sigma_1{}^2\sigma_3\omega_2$	0.076	9.3	1.3	−8.1
$\sigma_1{}^2\sigma_3{}^2\omega_2$	0.054	22.9	4.3	22.5
σ_1	0.046	2.0	2.4	1.6
$\sigma_1\sigma_3$	0.033	4.6	4.3	1.1
$\sigma_1\sigma_3$	0.033	11.6	1.9	2.5
$\sigma_1\sigma_3{}^2$	0.023	22.2	2.6	22.0

[a] There are two configurations for each entry. Units are D^2 for μ^2, $Å^6$ for γ^2, and 10^{10} cm^5 statvol^{-2} mol^{-1} for mK. [b] Ratio of the statistical weight to the configuration partition function, using the reference set of conformational energies and $T = 298$ K. Summation of the 16 statistical weights accounts for 90% of the configuration partition function.

weights of $\sigma_1{}^2\omega_2$ or $\sigma_1{}^2\sigma_3\omega_2$. Their μ^2 and γ^2 lie on either side of the average value, causing $\langle \mu^2 \rangle$ and $\langle \gamma^2 \rangle$ to vary little with $E_{\sigma 1}$. The molar Kerr constants for these same six configurations are either essentially zero or negative. Consequently $\langle mK \rangle$ increases as $E_{\sigma 1}$ increases (Figure 11). The experimental $\langle mK \rangle$ requires that $E_{\sigma 1}$ be negative. A value of −0.5 kcal/mol is selected as the reference value.

Calculated $\langle \mu^2 \rangle$ and $\langle mK \rangle$ are extremely sensitive to $E_{\sigma 3}$, as shown in Figure 12. Four of the 16 configurations listed in Table III have statistical weights which include $\sigma_3{}^2$. These
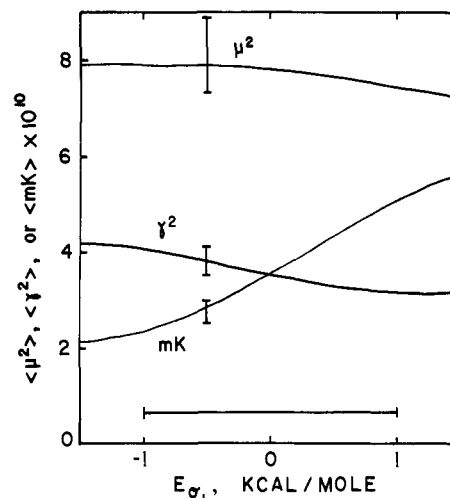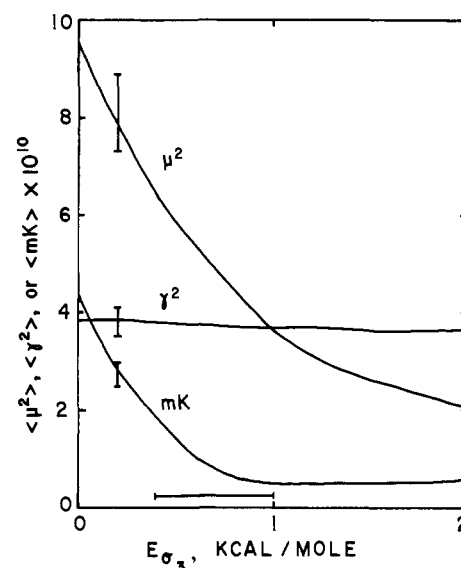
configurations are characterized by large values of μ^2 and mK. Hence $\langle \mu^2 \rangle$ and $\langle mK \rangle$ decrease rapidly as $E_{\sigma 3}$ increases from zero. Experimental values require that $E_{\sigma 3}$ be no larger than about 0.2 kcal/mol. Somewhat higher energies were suggested by the conformational energy calculations. However, it must be recalled that the computed energy arises not from a single interaction, but rather as the sum of four 6–12 interactions plus a small contribution from a torsional potential. Apparently the net interaction is less repulsive than the conformational energy calculations suggest.

There is a strong correlation in effects produced by variation in $E_{\sigma 3}$ and θ_μ, as demonstrated by Figures 5 and 12. Movement of θ_μ into its probable range would decrease $\langle \mu^2 \rangle$ and $\langle mK \rangle$ while producing no effect on $\langle \gamma^2 \rangle$. These changes could be compensated by a small decrease in $E_{\sigma 3}$. Thus use of $\theta_\mu = 63°$, in conjunction with $E_{\sigma 3} = 0.0$ kcal/mol, would yield $\langle \mu^2 \rangle$, $\langle \gamma^2 \rangle$, and $\langle mK \rangle$ within 3% of those calculated using the reference set.

None of the configurations listed in Table III has a statistical weight which includes σ_2, which explains the insensitivity of computed results to variation in $E_{\sigma 2}$ over its probable range.

The only ω_i appearing in Table III is ω_2. Variation in $E\omega_2$ produced trends which bear a qualitative resemblance to those

seen upon variation in E_{σ_1}. This result follows from the appearance of $\sigma_1{}^2\omega_2$ in the statistical weight of those configurations which have trans states for the first bonds in branches 2 and 3. The pertinent elements occur in the first column of $_2U_1$ θ_3U_1.

Altered distributions denoted by solid lines in Figures 8–10 are obtained using the reference statistical weights. In each case the distribution separates into three groups, the lowest population being in the group with the largest μ^2, γ^2, or mK. This change in distributions is achieved with little effect on $\langle\mu^2\rangle$ and $\langle\gamma^2\rangle$, but there is a significant decrease in $\langle mK\rangle$.

Comparison of Solid-State and Solution Configurations

Crystalline forms known as β-tricaprin[12] and β-trilaurin[29] contain similar conformations for the triglyceride. All dihedral angles in branches 1 and 2 occupy trans states. Branch 3 leaves the glycerol moiety perpendicular to the planar zigzag formed by branches 1 and 2. It then folds, primarily through a g^+ placement at $_3\phi_4$. This fold permits the hydrocarbon tail of branch 3 to run parallel to, and in contact with, the hydrocarbon portion of branch 2. This conformation has aptly been described as a "tuning fork."[12,29] For this conformation μ^2 is 1.7 D^2, while measured values for tripalmitin and tristearin in solution are 8.1 ± 0.8 D^2.[20–23] Clearly the solid-state configuration for the glycerol moiety, which merits a statistical weight of $\sigma_1\sigma_2$, cannot be dominant in solution. The reference set of statistical weights yields about 1% of the triacetin molecules in solution with values of $_1\phi_{n_1}$, $_2\phi_1$, $_2\phi_2$, $_3\phi_1$, and $_3\phi_2$ which correspond to those found for β-tricaprin and β-trilaurin in the crystalline state. The rotational isomeric state treatment is required to account for the configuration-dependent properties exhibited by triglycerides in solution.

References and Notes

(1) On sabbatical leave from Louisiana State University. Address correspondence to this author at the Department of Chemistry, Louisiana State University, Baton Rouge, La. 70803.
(2) Departamento de Quimica-fisica, Facultad de Ciencas, Universidad de Extremadura, Badajoz, Spain.
(3) E. Oldfield and D. Chapman, *FEBS Lett.*, **23**, 285 (1972).
(4) C. D. Linden and C. Fred Fox, *Acc. Chem. Res.*, **8**, 321 (1975).
(5) A. M. Scanu and C. Wisdom, *Annu. Rev. Biochem.*, **41**, 703 (1972).
(6) R. E. Jacobs, B. Hudson, and H. C. Anderson, *Proc. Natl. Acad. Sci. U.S.A.*, **72**, 3993 (1975).
(7) M. B. Jackson, *Biochemistry*, **15**, 2555 (1976).
(8) P. J. Flory, "Statistical Mechanics of Chain Molecules", Wiley, New York, N.Y., 1969.
(9) P. J. Flory, *Macromolecules*, **7**, 381 (1974).
(10) W. L. Mattice, *Macromolecules*, **8**, 644 (1975).
(11) W. L. Mattice, *Macromolecules*, **9**, 48 (1976).
(12) L. H. Jensen and A. J. Mabis, *Acta Crystallogr.*, **21**, 770 (1966).
(13) D. A. Brant, A. E. Tonelli, and P. J. Flory, *Macromolecules*, **2**, 228 (1969).
(14) A. Abe, R. L. Jernigan, and P. J. Flory, *J. Am. Chem. Soc.*, **88**, 631 (1966).
(15) E. Saiz and P. J. Flory, in preparation.
(16) J. E. Piercy and S. V. Subrahmanyam, *J. Chem. Phys.*, **42**, 1475 (1965).
(17) J. McAlister, N. Yathindra, and M. Sundaralingam, *Biochemistry*, **12**, 1189 (1973).
(18) J. E. Mark and P. J. Flory, *J. Am. Chem. Soc.*, **87**, 1415 (1965).
(19) J. E. Mark and P. J. Flory, *J. Am. Chem. Soc.*, **88**, 3702 (1966).
(20) W. N. Stoops, *J. Phys. Chem.*, **35**, 1704 (1931).
(21) S. D. Gokhale, N. L. Phalnikar, and S. B. Dhave, *J. Univ. Bombay A*, **11**, 56 (1943).
(22) N. N. Stepanenko and V. Agranat, *J. Exp. Theor. Phys. (USSR)*, **14**, 226 (1944).
(23) N. N. Stepanenko, B. A. Agranat, and T. Novikova, *Acta Physicochem. URSS*, **20**, 923 (1945).
(24) G. D. Patterson and P. J. Flory, *J. Chem. Soc., Faraday Trans. 2*, **68**, 1098 (1972).
(25) C. W. Carlson and P. J. Flory, *J. Chem. Soc., Faraday Trans. 2*, **73**, 1505 (1977).
(26) E. Saiz, U. W. Suter, and P. J. Flory, *J. Chem. Soc., Faraday Trans. 2*, **73**, 1538 (1977).
(27) In preparation.
(28) U. W. Suter and P. J. Flory, *J. Chem. Soc., Faraday Trans. 2*, **73**, 1521 (1977).
(29) K. Larrson, *Ark. Kemi*, **23**, 1 (1964).

# Dynamics of Light-Induced Redox Processes in Microemulsion Systems

J. Kiwi and M. Grätzel*

Contribution from the Institut de Chimie Physique, Ecole Polytechnique Fédérale, Lausanne, Switzerland. Received January 18, 1978

Abstract: Photoredox processes of the kind shown in eq 1 were investigated in oil/water microemulsions (water content >80%) by means of laser photolysis and steady-state illumination techniques. The following two redox couples were employed: (1) A = duroquinone (DQ), D = diphenylamine (DPA), and (2) A = methylviologene (MV^{2+}), D = *N*-methylphenothiazine (MPTH). In the first system, the two reactants are both solubilized in the lipid interior of the microemulsion droplet. The electron transfer from DPA to photoexcited DQ was found to occur in two steps: a rapid subnanosecond reaction involving DQ singlet states and a slower triplet reaction occurring in the microsecond time range. The diphenylamine cation produced associates with parent DPA molecules to yield multimer complexes. This process is controlled by the statistics of probe distribution among the droplets. A detailed account of the kinetics of formation and spectral characteristics of the multimers is given. In the second system, the electron transfer occurs from MPTH excited states inside the droplet to MV^{2+} which is absorbed on the droplets' surface. It exhibits also a fast (nanosecond) and a slower (microsecond) component resulting from the reaction of singlet and triplet states. The fate of the radical ions produced is examined and photobiological implications are discussed.

Introduction

Photoinduced electron transfer reactions of the type

$$A + D \underset{\Delta}{\overset{h\nu}{\rightleftharpoons}} A^- + D^+ \qquad (1)$$
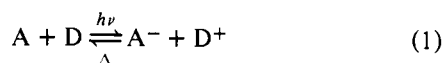
where A and D stand for the acceptor and donor, respectively, have recently attracted attention as potentially useful systems to convert light into chemical energy. The reversible character of process 1 has been a major obstacle in the practical utilization of these systems. Reactions that are endoergic in the